Desalination and Water Treatment
www.deswater.com

doi:10.5004/dwt.2019.23709

145 (2019) 211–219
March

A bimetallic (copper/cobalt) embedded poly (acrylamide) hydrogel for the synergistic catalytic degradation of methylene blue dye

Tallal Bin Aftab, Asif Hussain, Fei Xue, Dengxin Li*

College of Environmental Science and Engineering, State Environmental Protection Engineering Center for Pollution Treatment and Control in Textile Industry, Donghua University, 2999 Renmin Road, Shanghai 201620, China, Tel. +86-18601700705, email: tallal@live.com (T.B. Aftab), Tel. +86-13122194207, email: asif.fuuast@hotmail.com (A. Hussain), Tel. +86-15202167352, email: xuefeiwin@outlook.com, (F. Xue), Tel. +86-13636641041, email: lidengxin@mail.dhu.edu.cn (D. Li)

Received 15 July 2018; Accepted 28 December 2018

ABSTRACT

Herein, the synergistic catalytic degradation efficiency of polyacrylamide hydrogel embedded with copper and cobalt ions was studied over methylene blue (MB) dye. The morphology of the bimetallic hydrogel was analyzed by FTIR, SEM, and EDX. Fourier transform infrared spectroscopy (FTIR) was used to investigate the chemical composition. To explore the efficiency of CuCo@PAM catalyst for the MB dye degradation, all critical parameters such as mass, dye concentration, H_2O_2, temperature, and pH were studied and optimized. The maximum MB oxidative catalytic efficiency, under optimal conditions, for bimetallic hydrogel (CuCo@PAM) was found to be 97% which was 23% more than Cu@PAM and 17.9% more than Co@PAM, for hydrogel with copper was 74% and hydrogel with cobalt was 79.1%. Therefore, this signifies the synergistic catalytic degradation characteristics exhibited by the bimetallic hydrogel (CuCo@PAM). Based on the experimental results, the regression analysis was conducted for the catalytic degradation of MB dye process. The stability and reusability catalyst was achieved up to three consecutive cycles.

Keywords: Hybrid; Catalysis; Dye wastewater; Bimetal catalyst; Polyacrylamide

1. Introduction

The globalization and industrialization in last few decades, have adversely affected the water streams and ultimately affected the ecological system. This is currently, one of the most burning environmental issues. The complexes which are causing the water pollution, have a wide range of composition and have very toxic effects. Amongst them, are the by-products of textile industries, textile dyes, pharmaceutical, food-stuff, cosmetic, paper, leather industries, etc. most of the dyes colorize the water at very low concentrations (even at 1 mg L^{-1}), causing serious ecological implications on the natural water resources, as the textile dyes wastewater is mostly discharged in nature without treatment. Moreover, the textile wastewater has disastrous effects on the aqua-marine life, inhibiting their photosynthesis activity of the marine flora [1,2].

These dyes have a very high chemical and photo resistance, which creates a potential threat of bioaccumulation and therefore has serious health implications for humans through the food chain. Therefore, the treatment of textile dyes wastewater, prior to their discharge in natural water resources is of utmost importance, but the processes involved are very complicated.

The hydrogels possess a three-dimensional, flexible polymeric network, that allows them to absorb a huge amount of water from the aqueous environment [3–5]. The functionalized hydrogels have been extensively used in various applications, owing to diverse applications in drug release, water treatment, and biosensors. Moreover, the hydrogels, have also been applied as super adsorbents [6–8], as membranes in separation and desalination and have also been they considerably used in other numerous applications [9]. The extraordinary flexible characteristics of hydrogels, allows them to be modified accordingly. The metal embedded hydrogels prevent crystal growth, catalyst

*Corresponding author.

deactivation, and coalescence. These unique characteristics of hydrogels, allows them to be synthesized in-situ by cross-linking the gel with all kinds of metallic ions. Recently, great attention has been attracted in developing the synthesis of metal–polymeric hydrogel nanocomposites through in-situ reduction of metal ions, which is formerly adsorbed onto polymeric hydrogels [10–12].

Very few studies have so far been conducted to use the metal embedded hydrogels for the degradation of the textile dyes. Most of the researchers conducted so far is based on the application of metal embedded hydrogel composites on either catalytic reduction or hydrogen production [9–11,13,14].

One of the most colored and commonly used textile dye is methylene blue (MB). It is mostly used for wood, ying cotton, and silk. It's a toxic compound which can cause permanent burns to human and animals, vomiting, nausea, excess sweating, mental confusion and methemoglobinemia [15]. Therefore, MB dye removal from wastewater has caught the considerable attention of the researchers in the field of environmental pollution.

For the treatment of wastewater, the advanced oxidation processes (AOP's) have attracted significant attention as they can generate highly powerful chemical substances ($^{\bullet}OH$, $O_2^{\bullet -}$, etc.). one of the most commonly used methods in AOP's is called the Fenton process (dissolved Fe(II) and H_2O_2) [16], which has a tendency to degrade organic contaminants into harmless chemicals like CO_2 and H_2O. Nonetheless, the Fenton reactions application is very limited for the following reasons: It only works on pH < 4 [17,18] separation and recovery of the iron ions especially in industrial wastewater treatment [19], to overcome these shortcomings, substantial efforts have been made for the development of heterogeneous Fenton systems [20,21] and so far a number of heterogeneous Fenton-like catalysts have been reported, like iron oxides [22–26], iron-immobilized zeolites [27], clays [28], and carbon compounds [29,30] compared to traditional Fenton catalyst, the heterogeneous catalysts can effectively work over a wide range of pH for the oxidative degradation of organic pollutants.

The aim of this research is to explore the degradation ability of the bimetallic hydrogel having copper and cobalt ions embedded in the hydrogel (CuCo@PAM), using H_2O_2 as an oxidant, for the degradation of MB dye. The bimetallic hydrogel was produced following the free radical polymerization method. The resulting bimetallic hydrogel catalyst (CuCo@PAM) was found to be highly effective for the degradation of MB with H_2O_2 as oxidant at neutral pH and also after three consecutive cycles, its reusability was found to be very effective with a very low change in MB dye degradation efficiency. So far, no studies have been reported for the catalytic degradation of MB dye using a CuCo@PAM (bimetallic hydrogel).

2. Material and methods

2.1. Material

Acrylamide (AM), N,N-methylenebis (acrylamide), copper(II) nitrate trihydrate ($Cu(NO_3)_2{\cdot}3H_2O$), cobalt(II) nitrate hexahydrate ($Co(NO_3)_2{\cdot}6H_2O$), N,N-methylenebisacrylamide ($C_7H_{10}N_2O_2$) (MBA) purchased from Sigma–Aldrich, sodium hydroxide (NaOH), ammonium persulfate (APS), N,N,N,N-tetramethylethylenediamine ($((CH_3)_2NCH_2CH_2N(CH_3)_2)$(TEMED), hydrazine monohydrate ($N_2H_4{\cdot}H_2O$) (80%) was used as reducing agent for in situ metal reduction, hydrogen peroxide (H_2O_2) (30%, w/w), methylene blue dye (MB), were supplied by Sinopharm Shanghai, China and were used without any further purification.

2.2. In-situ synthesis of copper and cobalt metals on PAM hydrogel

The free radical polymerization method was adopted for the synthesis of polyacrylamide (PAM) hydrogel, using N,N-methylene-bisacrylamide (MBA) as a cross-linker and APS/TEMED was used as a redox-initiating pair using the usual procedure [31]. 300 mg of acrylamide (AM) was dissolved in deionized water. Subsequently,the crosslinker MBA of 4 mg was added. When 15 mg of APS and 4 µL of TEMED were added to the mixture, the free radical polymerization was initiated. The solution rapidly turned highly viscous, and after few minutes a solid gel was obtained. The experiment was conducted at controlled temperature i.e. 25°C. For the completion of the polymerization reaction, the gel was kept for 24 h at 25°C. After 24 h, the gel was extracted from the container and was washed with deionized water to ensure the elimination of the unreacted compounds. Then PAM hydrogel was immersed in a solution having $Cu(NO_3)_2{\cdot}3H_2O$ and $Co(NO_3)_2{\cdot}6H_2O$, with a weight ratio of 1:1. After 24 h, the PAM metal embedded hydrogel was removed from the metal solution and was then kept in deionized water for another 12 h, to ensure the removal of free unbound metal ions. The filtered solid was immersed in 100 mL of ethylene glycol solution containing 0.5 M of $N_2H_4{\cdot}H_2O$ (hydrazine monohydrate) at 60°C for 6 h, to ensure the completion of the *in-situ* reduction process. Thereafter, the metal embedded hydrogel nanocomposite was decanted, washed with deionized water and subjected to freeze-drier [32]. The final product was stored in a closed container at ambient temperature.

2.3. Characterization of CuCo@PAM hydrogel

The Fourier transform infrared (FTIR) spectra were recorded over the range of 400–4000 cm^{-1} (NICOLET-6700, UK). The surface morphology of CuCo@PAM hydrogel was examined using the scanning electron microscopy (SEM) using (Quanta 250, USA) equipped with an energy-dispersive X-ray spectrometer (EDX) (X-Max 80, Aztec, Oxford).

2.4. Removal procedures of MB dye

During the experiments for the MB dye degradation, the residual MB concentration was measured using UV spectrophotometer (Shimadzu UV-spectrophotometer, UV- 1800) using absorbance at λ = 665 nm. These experiments were performed using 100 mL flasks. These flasks were sealed and agitated at 100 rpm in a thermostatic shaker maintained at variables temperature ranging from 25–55°C. The typical reaction mixture was initiated with 50 mL of dye at 100–400 mg L^{-1} having a hydrogel metal composite of 0.025–0.1 g. The catalytic oxidation of MB dye was carried out in a 100

mL flasks in the presence of H_2O_2. During the study for the effect of initial H_2O_2 on catalytic reaction, its amount was varied from 0.2–1.0 mL. To investigate the effect of initial pH on the reaction, the dye solution was adjusted from 3 to 9.2 mL. The samples were periodically withdrawn from the catalytic solution during the experiments and were measured immediately for the respective parameters. The reusability experiment of CuCo@PAM was executed with the optimal conditions for the degradation of MB dye. Dye removal percentage (%) was calculated using Eq. (1).

$$\text{Removal } \% = \frac{C_o - C_t}{C_o} \times 100 \quad (1)$$

where C_o (mg L^{-1}) and C_t (mg L^{-1}) represent the initial and final (t) time concentrations of MB dye in the solution.

3. Results and discussion

3.1. Characterization

The Fourier-transform infrared (FT-IR) spectrometry of No metals@PAM and CuCo@PAM was investigated. In Fig. 2, the spectra of (a) No metals@PAM and (b) CuCo@PAM, both exhibited many common bands, as both contained typical polyacrylamide bands [33,34] see Fig. 2. A broad band in the region 3000–3700 cm^{-1} appears in both the IR spectra, due to the OH stretching vibrations of absorbed water, hydroxyl group being H-bound, as the peak is very broad. A broad peak can be seen for No metals@PAM and CuCo@PAM at 3335 cm^{-1} and 3339 cm^{-1}, which are ascribed to hydroxyl asymmetrical stretching vibration and $–NH_2$ stretching vibration, respectively. The band which appears at 2931 cm^{-1} and 2953 cm^{-1}, for No metals@PAM and CuCo@PAM IR spectra, corresponds to C–H asymmetric stretch in CH_2 respectively. In both spectra typical amide C=O stretch at ~1652 cm^{-1} experienced no change which means that this group had no interaction with the in-situ deposited metals. The doublet is seen at 1413 cm^{-1} and 1450 cm^{-1} corresponds to the deformation vibration of –NH groups. In summary, corresponding to the stretching vibration of hydroxyl, amino and amide groups became weaker and sharper which indicated the strong interaction between these groups and copper or cobalt.

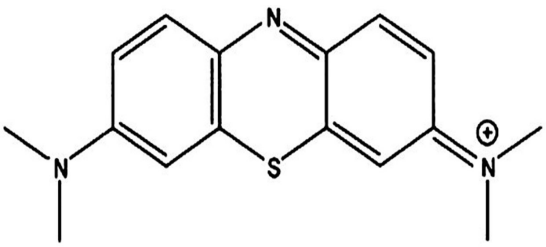

Fig. 1. Chemical structure of methylene blue (MB) dye.

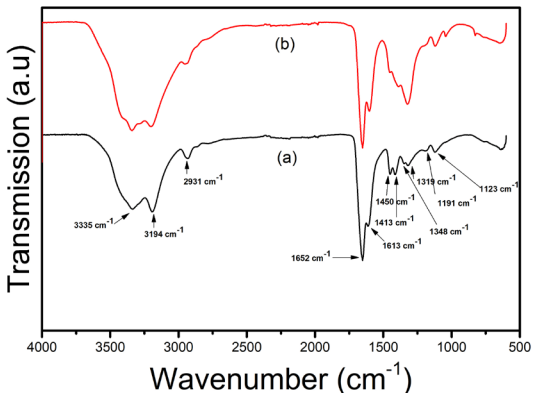

Fig. 2. FT-IR spectra (a) No metals@PAM and (b) CuCo@PAM.

The samples of CuCo@PAM were characterized by *scanning electron microscopy (SEM)* as seen in Fig. 3 at different magnifications. It illustrates that the spherical, bead-like shape of metal ions embedded in the hydrogel.

The *Energy-Dispersive X-rays spectroscopy (EDX)* directly revealed the existence of the metal ions of copper and cobalt embedded on the hydrogel. The identification of Cu and Co metal ions is confirmed by Fig. 4. The corresponding area is enclosed within a green line, Fig. 4. The mapping of this area is shown in Fig. 5 and is well consistent with the EDX spectra.

3.2. Optimization of catalytic system parameters

3.2.1. Effect of the mass of the catalyst

The mass of the catalyst is a significant aspect in the treatment of dye wastewater. In this study, the variation in mass was applied to the series of experiments, in order to study the correlation between the effect of the mass of the catalyst and the degradation efficiency of MB from the water. Variable masses of CuCo@PAM catalyst i.e. 0.025, 0.050, 0.075 and 0.1 g were applied to the MB dye wastewater.

During this experiment, the control parameters were as follows: 1.0 mL of H_2O_2 was added to the MB dye solution of 50 mL, MB dye concentration was 100 mg L^{-1}, pH was 7 and temperature was set at 25°C. When the CuCo@PAM mass was 0.025 g, the MB removal rate was 59.8% only. At mass equal to 0.050 g, the removal efficiency of the CuCo@PAM catalyst was found to be the greatest i.e. 90.7%. At mass equal to 0.075 and 0.10 g, the dye degradation efficiency was calculated at 88 and 89% respectively. The graphical results are presented in Fig. 6.

3.2.2. Effect of initial H_2O_2 dosage

During the catalysis, one of the most significant factors, is the dosage of H_2O_2 in the system. The effect of hydrogen

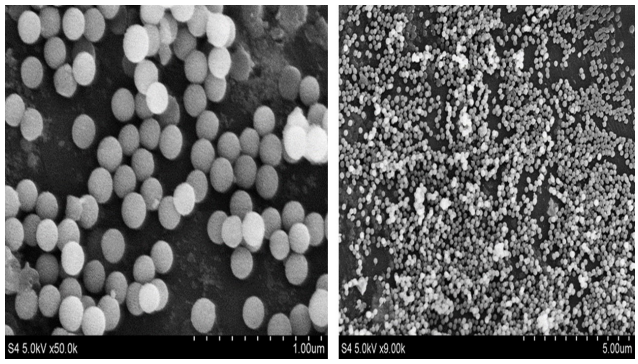

Fig. 3. SEM images of CuCo@PAM at different magnifications.

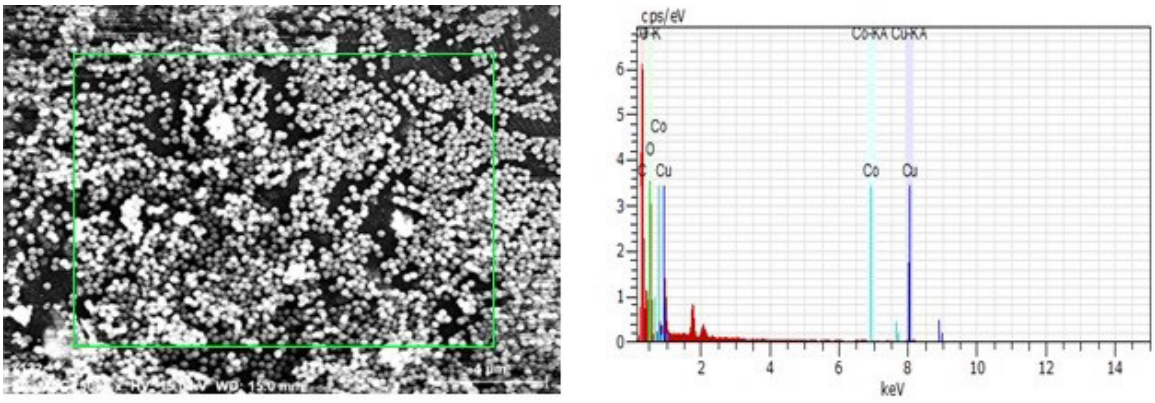

Fig. 4. EDX spectra of the corresponding SEM image area of CuCo@PAM.

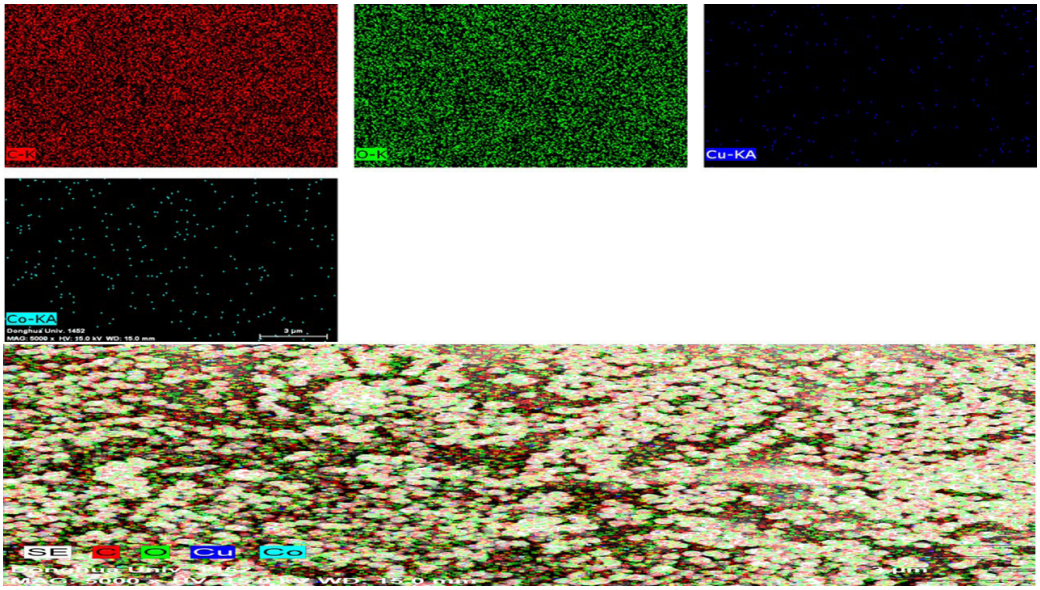

Fig. 5. EDX elemental mapping of the corresponding SEM image area of CuCo@PAM.

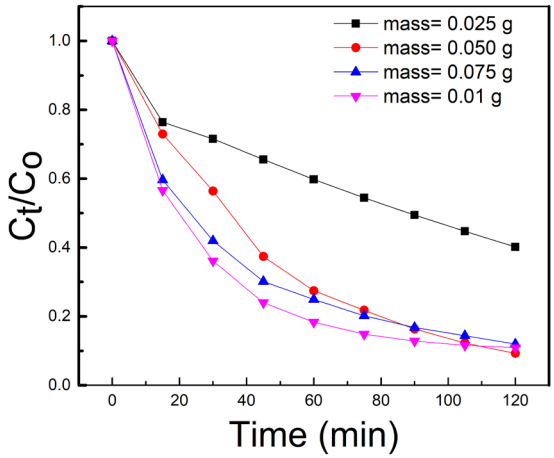

Fig. 6. The effect of the mass of CuCo@PAM on the degradation of MB dye. (T = 25°C, initial concentration 100 mg L^{-1}, 50 mL, 1.0 mL H_2O_2, pH = 7).

peroxide dosage was studied in the range of 0.2 mL to 1.0 mL (H_2O_2 30%) for 50 mL MB dye solution. The control variables in this study were as follows: the mass of CuCo@PAM was 0.05 g, MB dye concentration was 100 mg L^{-1}, pH was 7 and temperature was set at 25°C. In this experiment, it was found that the initial reaction rate increases, with the increase in hydrogen peroxide dosage and vice versa as presented in Fig. 7. As the H_2O_2 dose was increased from 0.2 mL to 1.0 mL the MB removal efficiency of CuCo@PAM exhibited a sharp increase. At 0.2, 0.4, 0.6, 0.8 and 1.0 mL of H_2O_2 dose, the removal efficiencies were calculated to be 73.46, 79, 79.2, 84 and 93 % respectively. Based on these results, the optimal dose was found to be 1.0 mL, with the mass of the catalyst at 0.05 g, dye concentration 100 mg L^{-1}, temperature 25°C and pH 7. The graphical illustration can be seen in Fig. 7.

3.2.3. *Effect of initial dye concentration*

After the optimization of the mass of the CuCo@PAM gel (0.05 g), the H_2O_2 dosage (1.0 mL) and temperature (25°C),

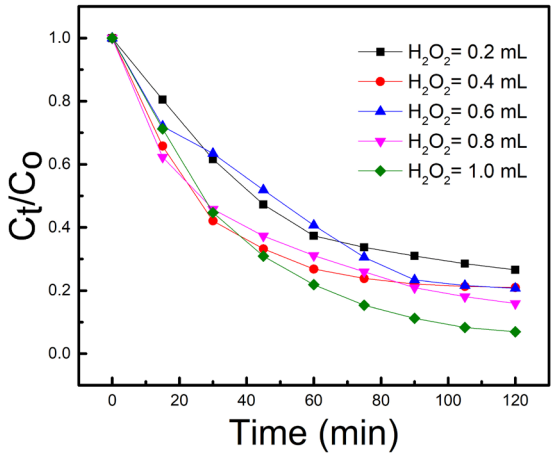

Fig. 7. The effect of the initial dose of H_2O_2 on the degradation of MB dye. (Mass 0.05 g, T = 25°C, initial concentration 100 mg L^{-1}, 50 mL, pH = 7).

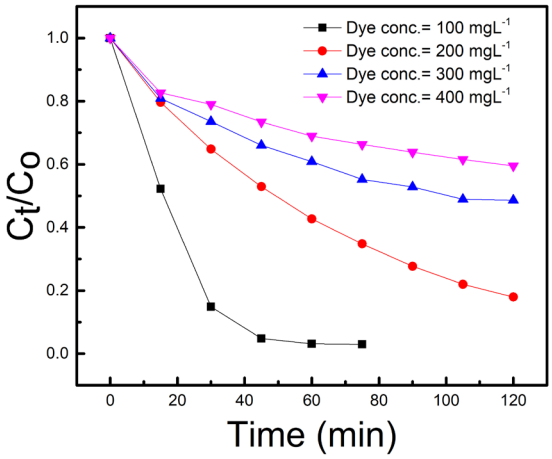

Fig. 8. The effect of the initial MB dye concentration on the degradation of MB dye. (Mass 0.05 g, T = 25°C, dye sol. vol = 50 mL, 1.0 mL H_2O_2, pH = 7).

the next parameter to optimize was the initial dye concentration. The catalytic decolorization of MB dye was conducted by varying the initial concentrations of the dye from 100 mg L^{-1} to 400 mg L^{-1} in order to assess the efficiency of the catalyst at different MB dye concentrations and to find the optimal value. The experimental results indicated that not only removal rates of CuCo@PAM exhibited a decline as the MB dye concentrations were increased, but also, the time period required for the degradation was increased. The efficiency at 100, 200, 300 and 400 mg L^{-1} were 97, 82, 51.3 and 40.4 % respectively. Therefore, the optimal MB dye concentration for MB degradation was found to be 100 mg L^{-1} with mass 0.05 g, H_2O_2 1.0 mL, pH 7 and temperature 25°C. The graphical details are shown in Fig. 8.

3.2.4. pH Sensitivity of CuCo@PAM catalyst

For the treatment of wastewater, the pH plays a critical role, hence the variation in the pH of the wastewater should be focused. Its significance has the following reasons. One is that the discharged wastewater from the industries has a wide range of pH values. The other reason for this is that the pH conditions are directly affected by the generation of hydroxyl radicals [33].

To study the effects of pH, for the degradation of MB dye, the catalytic degradation experiments were conducted in order to evaluate the efficiency of CuCo@PAM at pH values of 3, 5, 7 and 9. The degradation efficiency of MB dye for different pH values is shown in Fig. 9. It was observed that the MB dye degradation by CuCo@PAM increased significantly with the decrease of pH from 7 to 3 and decreased with the increase in pH after 9. Further, it can be observed from Fig. 9 that the reaction can advance at a wider pH range from acidic to alkaline this catalytic degradation system (Fig. 9). Although, the lower pH resulted in higher oxidation rate. This outcome is unique from the Fenton system, in which, the oxidation can only take place at pH lower than 3. In this study, for pH 5–7, the removal rates for MB were 94 and 97% respectively. At pH 9 the removal efficiency was 96.1%. Therefore, the optimal pH for the MB removal was found to be 7. However lower pH values (pH 5 and 6) were found to be the most favorable for the catalytic oxidation of the MB dye.

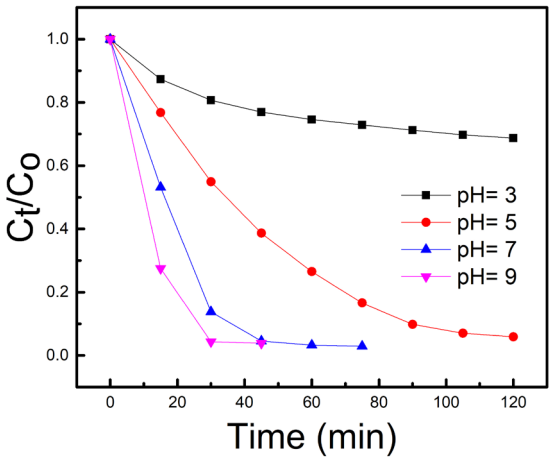

Fig. 9. The effect of the initial pH on the degradation of MB dye. (Mass 0.05 g, T = 25°C, initial concentration 100 mgL^{-1}, 50 mL, 1.0 mL H_2O_2).

3.2.5. Effect of reaction temperature

Fig. 10, demonstrates the degradation rate of the MB dye, as a function of time at variable temperatures. The degradation rate of MB dye was less at low-temperature (Fig. 10) and displayed an increasing trend as the temperature was increased. The experiment was investigated on a range of temperatures, i.e. 25, 35, 45 and 55°C. The control parameters were as follows: the mass of CuCo@PAM was 0.05 g, MB dye concentration was 100 mg L^{-1}, pH was 7 and the H_2O_2 dose was 1.0 mL. As the temperature was raised, a sharp increase in the rate of MB dye degradation was observed. The MB dye removal efficiencies at 25, 35, 45 and 55°C were 90.7, 97, 96.2 and 96.89% respectively. As

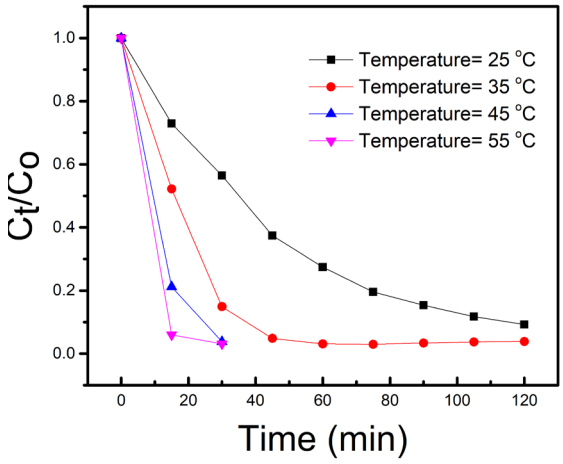

Fig. 10. Effect of the reaction temperature on the degradation of MB dye. (Mass 0.05 g, initial concentration 100 mg L^{-1}, 50 mL, 1.0 mL H_2O_2, pH = 7).

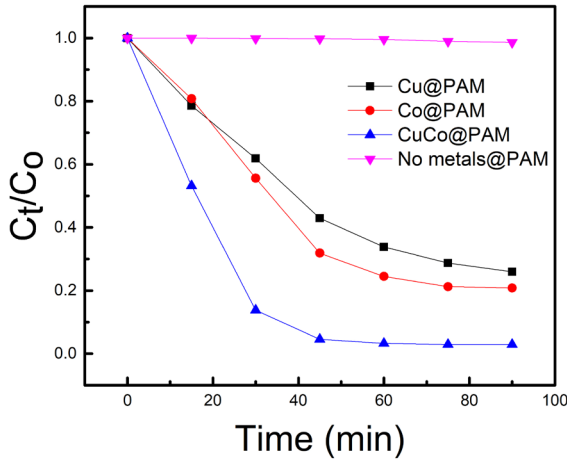

Fig. 11. The effect of the various catalysts on the degradation rate of MB dye. (Mass 0.05 g, T = 35°C, initial concentration 100 mg L^{-1}, 50 mL, 1.0 mL H_2O_2, pH = 7).

shown in Fig. 10, that degradation efficiency of CuCo@PAM for MB dye, under the influence of H_2O_2, increased with the increase in temperature from 25 to 35°C. When the reaction temperature was further increased up to 45°C and 55°C, it resulted in a very small decline in degradation efficiency, as compared to the efficiency at 35°C. But the increase in temperature also resulted in rapid degradation of MB dye at 45°C and 55°C. When the temperature is raised above 35°C, the H_2O_2 utilization efficiency starts to decline. This is because of the exponential disintegration of H_2O_2 into oxygen and water. Thus, the optimum temperature for most effective oxidative degradation of dyes with H_2O_2 as an oxidant is in the range of 30–35°C [34]. These results are evidence that the optimal temperature for this experiment was found to be 35°C with other optimal conditions as follows: mass 0.05 g, dye concentration 100 mg L^{-1}, H_2O_2 1.0 mL and pH 7.

3.3. Comparison between no metals@PAM, Cu@PAM, Co@PAM and CuCo@PAM catalysts for MB degradation

To analyze the performance of the bimetallic CuCo@PAM catalyst, a comparative study was conducted in order to find the MB dye removal efficiency in comparison with No metals@PAM, Cu@PAM, and Co@PAM catalysts. The control parameters for these three catalysts were as follows: the mass of the catalyst was 0.05 g, H_2O_2 was 1.0 mL, the temperature was 35°C, dye concentration was 100 mg L^{-1} and the pH was 7. As seen from Fig. 11, the most efficient catalyst was the CuCo@PAM, as its removal efficiency was found to be 97% within 75 min. For No metals@PAM, a total of 1.5% removal rate was observed after 120 min. In the case of Cu@PAM catalyst, the removal efficiency was only 74% in 90 min. However, for Co@PAM catalyst, the removal efficiency was relatively better than Cu@PAM catalyst i.e. 79.15% in 90 min. Therefore, from the aforementioned results, under the optimal control conditions, CuCo@PAM catalyst proved to be highly efficient than those of single metal catalysts and it exhibited a synergistic effect between the two metal ions (Cu and Co)embedded on the gel.

Table 1
The pseudo-first-order model corresponding to variable catalysts used for MB dye degradation

Catalyst type	MB dye removal (%)	K (min^{-1})	R^2
No metals@PAM	1.5	0.0002	0.9211
Cu@PAM	74	0.0159	0.9779
Co@PAM	79	0.0195	0.9371
CuCo@PAM	97	0.0498	0.9848

3.4. Kinetic isotherm studies

For present catalytic MB dye degradation studies, pseudo-first-order reaction kinetics were studied. Based on the first order reaction kinetics, the regression analysis was conducted for the catalytic degradation of MB dye process and the results are shown in Table 1. The regression coefficients (R^2) of No metals@PAM, Cu@PAM, Co@PAM, and CuCo@PAM were found be 0.9211, 0.9779, 0.9371 and 0.9848 respectively. Comparing the regression coefficients obtained from Table 1, it can be seen that based on the pseudo-first-order reaction kinetics the R^2 is highest for CuCo@PAM i.e. 0.9848. The graphical illustration has been presented in Fig. 12. The estimated kinetic rate constant (k) for No metals@PAM, Cu@PAM, Co@PAM and CuCo@PAM were found be in order of: 0.0002 (No metals@PAM) < 0.0159(Cu@PAM) < 0.0195(Co@PAM) < 0.0498(CuCo@PAM).

3.5. Proposed reaction mechanism

Our proposed reaction mechanism for the catalytic degradation of MB dye, by the application of CuCo@PAM, could be strongly supported by previous oxidative catalytic degradation studies [35–38]. The stepwise mechanism has been elaborated in Fig. 13 and Eqs. (2)–(6).

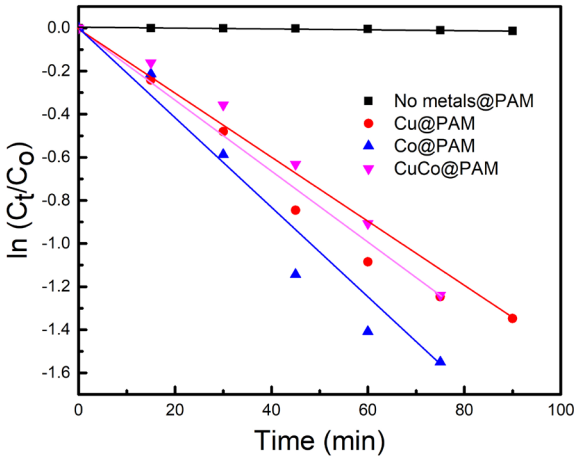

Fig. 12. Fitting curve of MB dye degradation with pseudo-first-order model. (Mass 0.05 g, T = 35°C, initial concentration 100 mg L^{-1}, 50 mL, 1.0 mL H_2O_2, pH = 7).

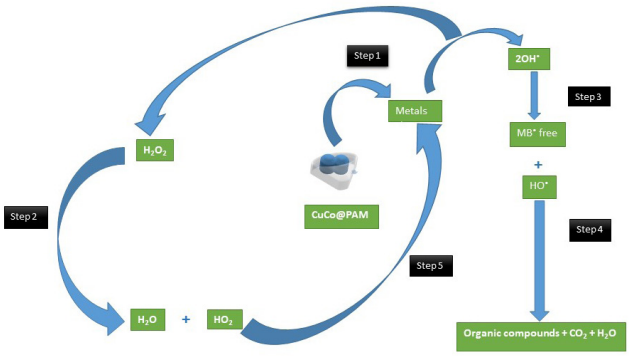

Fig. 13. Schematic illustration of the possible mechanism of MB dye degradation using CuCo@PAM under H_2O_2.

$$\text{Step1:}\quad \text{Metals} + H_2O_{2(aq)} = \text{Metals}^{n+} + HO^-_{(aq)} + HO^{\bullet}_{(aq)} \qquad (2)$$

$$\text{Step 2:}\quad HO^{\bullet}_{(aq)} + H_2O_{2(aq)} = HO_2^{\bullet}{}_{(aq)} + H_2O\ (\text{liq}) \qquad (3)$$

$$\text{Step 3:}\quad HO^{\bullet}_{(aq)} + MB_{\text{free}} \rightarrow H_2O_{(aq)} + MB^{\bullet}_{\text{free}} \qquad (4)$$

$$\text{Step 4:}\quad MB^{\bullet}_{\text{free}} \rightarrow \text{Organic compounds} + CO_{2\,(g)} + H_2O_{(\text{liq})} \qquad (5)$$

$$\text{Step 5:}\quad HO_2^{\bullet}{}_{(aq)} + \text{Metals}^{n+} = \text{Metals} + H^+\,(aq) + O^2{}_{(g)} \qquad (6)$$

The bimetallic ions in the hydrogel matrix, with a pseudo-first-ordered profile, degrade the MB dye by utilizing the hydroxyl radicals (HO•). As shown by Eqs. (2)–(6) the hydroxyl radicals (HO•) produced, react with dye molecules at the expense of formation of peroxide radicals ($HO_2^{\bullet}$) producing methylene blue chain radicals (MB). There seems to be a negative correlation in the concentration of the peroxide radicals and exhausted metallic ions [step 5, Eq. (6)]. Methylene blue chain radicals ($MB^{\bullet}_{free}$) further, generate organic compounds with CO_2 and H_2O. This reaction continues as the $HO_2^{\bullet}$ radicals advance towards the oxidized metals (metals $^{n+}$) to again convert them in reduced form

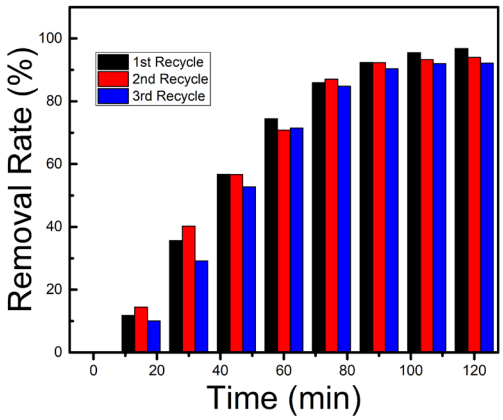

Fig. 14. Effect of the catalyst reusability on the catalytic degradation of removal percentage. (Mass 0.05 g, T = 35°C, initial concentration 100 mg L^{-1}, 50 mL, 1.0 mL H_2O_2, pH = 7).

(metals) and this reaction continues as a chain reaction. In this MB dye degradation process, most of the reactions are happening simultaneously. They have been split up in order to have a clear understanding. In this chain reaction, step 5 plays a key role. Therefore, it can be concluded that the catalytic degradation of MB dye by H_2O_2 is only performed through the generation of MB chain radicals from the reactions between hydroxyl radicals and dye molecules.

The synergistic characteristics of bimetallic complexes were reported by Han and coworkers. They prepared bimetallic Cu–Fe AO–PAN complex, which exhibited high degradation activity and stability for the oxidative degradation of the dye because of the existence of the synergetic effect. Therefore, the synergetic effect in Cu–Fe bimetal AO–PAN complexes is considered as the combined action of copper and iron ions facilitating the Fe^{3+}/Fe^{2+} cycle and exciting the Cu^{2+}/Cu^{+} redox, followed by the increase in the OH radical generation [39]. Subsequently, our CuCo@PAM hydrogel exhibited high MB dye degradation catalytic efficiency as compared to a single metal catalyst i.e. Cu@PAM and Co@PAM. Thereby, it is considered as the joint action of Cu and Co metallic ions, that signifies the synergistic catalytic characteristics of our CuCo@PAM catalyst.

3.6. Reusability

The stability and reusability of CuCo@PAM hydrogel were further demonstrated by the descriptive color changes of CuCo@PAM after three consecutive cycles of catalytic MB dye degradation. As seen in Fig. 14, the MB dye degradation results for 1st, 2nd and 3rd recycle for CuCo@PAM were 96.81, 94.04 and 92.16% respectively.

4. Conclusion

The bimetallic hydrogel CuCo@PAM was successfully synthesized and applied for the synergetic catalytic degradation of the MB dye under H_2O_2. The metallic Cu and Co ions were successfully embedded on the hydrogel. The morphological aspects of the CuCo@PAM catalyst were analyzed using FT-IR, SEM and EDX analysis. The CuCo@PAM

exhibited promising oxidative catalytic oxidation of the MB dye under optimized conditions. Our bimetallic CuCo@PAM exhibited a remarkable performance, as it degraded 97% of the MB dye within 75 min under the optimized conditions. Moreover, the catalytic oxidative mechanism for MB dye was also proposed in this study. The kinetic study indicated that the degradation kinetics of MB dye followed the pseudo-first-order kinetics. Its high efficiency, technical feasibility, and cost-effectiveness make it a very attractive dye removal treatment. The catalytic oxidation mechanism of the dyes removal further needs to be researched.

Declaration of interests

The authors report no conflicts of interest. The authors alone are responsible for the content and writing of this article.

Acknowledgment

This research work was financially supported by the national natural science Foundation in China (U1660107), Textile light application basic research in China (J201503) and Specialized research fund for the Doctoral Program of Senior Education in China (Grant No. 20130075110006).

References

[1] J. Zhang, K.-H. Lee, L. Cui, T.-s. Jeong, Degradation of methylene blue in aqueous solution by ozone-based processes, J. Ind. Eng. Chem., 15 (2009) 185–189.
[2] S. Lambert, N. Graham, C. Sollars, G. Fowler, Evaluation of inorganic adsorbents for the removal of problematic textile dyes and pesticides, Water Sci. Technol., 36 (1997) 173–180.
[3] U.P. Shinde, B. Yeon, B. Jeong, Recent progress of in situ formed gels for biomedical applications, Progr. Polym. Sci., 38 (2013) 672–701.
[4] S.C. Tang, P. Wang, K. Yin, I.M. Lo, Synthesis and application of magnetic hydrogel for Cr (VI) removal from contaminated water, Environ. Eng. Sci., 27 (2010) 947–954.
[5] G. Jing, L. Wang, H. Yu, W.A. Amer, L. Zhang, Recent progress on study of hybrid hydrogels for water treatment, Colloids Surfaces A: Physicochem. Eng. Asp., 416 (2013) 86–94.
[6] M.A. Mekewi, A.S. Darwish, Elaboration of metal (M: Co, Cu, Ni, Fe) embedded poly (acrylic acid-co-acrylamide) hydrogel nanocomposites: An attempt to synthesize uncommon architectured "Auto-active" nanocatalysts for treatment of dyeing wastewater, Mater. Res. Bull., 70 (2015) 607–620.
[7] N. Sahiner, O. Ozay, N. Aktas, D.A. Blake, V.T. John, Arsenic (V) removal with modifiable bulk and nano p (4-vinylpyridine)-based hydrogels: the effect of hydrogel sizes and quarternization agents, Desalination, 279 (2011) 344–352.
[8] S. Shirsath, A. Hage, M. Zhou, S. Sonawane, M. Ashokkumar, Ultrasound assisted preparation of nanoclay Bentonite-FeCo nanocomposite hybrid hydrogel: a potential responsive sorbent for removal of organic pollutant from water, Desalination, 281 (2011) 429–437.
[9] N. Sahiner, O. Ozay, E. Inger, N. Aktas, Superabsorbent hydrogels for cobalt nanoparticle synthesis and hydrogen production from hydrolysis of sodium boron hydride, Appl. Catal. B: Environ., 102 (2011) 201–206.
[10] S. Butun, N. Sahiner, A versatile hydrogel template for metal nano particle preparation and their use in catalysis, Polymer, 52 (2011) 4834–4840.
[11] N. Sahiner, S. Butun, O. Ozay, B. Dibek, Utilization of smart hydrogel–metal composites as catalysis media, J. Colloid Interface Sci., 373 (2012) 122–128.
[12] H. Won, H. Nersisyan, C. Won, Cobalt powders and porous cobalt particles prepared by co-reduction of hydrazine and sodium phosphate and its formation mechanism, Mater. Chem. Phys., 133 (2012) 225–231.
[13] F. Seven, N. Sahiner, Poly (acrylamide-co-vinyl sulfonic acid) p (AAm-co-VSA) hydrogel templates for Co and Ni metal nanoparticle preparation and their use in hydrogen production, Int. J. Hydrogen Energy, 38 (2013) 777–784.
[14] S. Sagbas, N. Sahiner, A novel p (AAm-co-VPA) hydrogel for the Co and Ni nanoparticle preparation and their use in hydrogel generation from $NaBH_4$, Fuel Process. Technol., 104 (2012) 31–36.
[15] M. Rafatullah, O. Sulaiman, R. Hashim, A. Ahmad, Adsorption of methylene blue on low-cost adsorbents: a review, J. Hazard. Mater., 177 (2010) 70–80.
[16] F. Harber, J. Weiss, The catalytic decomposition of hydrogen peroxide by iron salts, Proc. R. Soc. Lond. A, 147 (1934) 332–351.
[17] D.L. Sedlak, A.W. Andren, Oxidation of chlorobenzene with Fenton's reagent, Environ. Sci. Technol., 25 (1991) 777–782.
[18] J.J. Pignatello, Dark and photoassisted iron (3+)-catalyzed degradation of chlorophenoxy herbicides by hydrogen peroxide, Environ. Sci. Technol., 26 (1992) 944–951.
[19] S. Parra, I. Guasaquillo, O. Enea, E. Mielczarski, J. Mielczarki, P. Albers, L. Kiwi-Minsker, J. Kiwi, Abatement of an azo dye on structured C-Nafion/Fe-ion surfaces by photo-Fenton reactions leading to carboxylate intermediates with a remarkable biodegradability increase of the treated solution, J. Phys. Chem. B, 107 (2003) 7026–7035.
[20] H. Lim, J. Lee, S. Jin, J. Kim, J. Yoon, T. Hyeon, Highly active heterogeneous Fenton catalyst using iron oxide nanoparticles immobilized in alumina coated mesoporous silica, Chem. Commun., (2006) 463–465.
[21] J. He, W. Ma, J. He, J. Zhao, C.Y. Jimmy, Photooxidation of azo dye in aqueous dispersions of H_2O_2/α-FeOOH, Appl. Catal. B: Environ., 39 (2002) 211–220.
[22] R.C. Costa, M. Lelis, L. Oliveira, J. Fabris, J.D. Ardisson, R. Rios, C. Silva, R. Lago, Novel active heterogeneous Fenton system based on Fe_3–xMxO_4 (Fe, Co, Mn, Ni): the role of M^{2+} species on the reactivity towards H_2O_2 reactions, J. Hazard. Mater., 129 (2006) 171–178.
[23] F. Magalhães, M. Pereira, S. Botrel, J. Fabris, W. Macedo, R. Mendonca, R. Lago, L. Oliveira, Cr-containing magnetites Fe_3–x$CrxO_4$: the role of Cr^{3+} and Fe^{2+} on the stability and reactivity towards H_2O_2 reactions, Appl. Catal. A: General, 332 (2007) 115–123.
[24] L.C. Oliveira, T.C. Ramalho, E.F. Souza, M. Gonçalves, D.Q. Oliveira, M.C. Pereira, J.D. Fabris, Catalytic properties of goethite prepared in the presence of Nb on oxidation reactions in water: computational and experimental studies, Appl. Catal. B: Environ., 83 (2008) 169–176.
[25] A.C. Silva, D.Q. Oliveira, L.C. Oliveira, A.S. Anastacio, T.C. Ramalho, J.H. Lopes, H.W. Carvalho, C.E.R. Torres, Nb-containing hematites Fe_2–x$NbxO_3$: the role of Nb^{5+} on the reactivity in presence of the H_2O_2 or ultraviolet light, Appl. Catal. A: General, 357 (2009) 79–84.
[26] S. Yang, H. He, D. Wu, D. Chen, X. Liang, Z. Qin, M. Fan, J. Zhu, P. Yuan, Decolorization of methylene blue by heterogeneous Fenton reaction using Fe_3–x$TixO_4$ ($0 \le x \le 0.78$) at neutral pH values, Appl. Catal. B: Environ., 89 (2009) 527–535.
[27] M. Kasiri, H. Aleboyeh, A. Aleboyeh, Degradation of Acid Blue 74 using Fe-ZSM5 zeolite as a heterogeneous photo-Fenton catalyst, Appl. Catal. B: Environ., 84 (2008) 9–15.
[28] B. Iurascu, I. Siminiceanu, D. Vione, M. Vicente, A. Gil, Phenol degradation in water through a heterogeneous photo-Fenton process catalyzed by Fe-treated laponite, Water Res., 43 (2009) 1313–1322.
[29] J.H. Ramirez, F.J. Maldonado-Hódar, A.F. Pérez-Cadenas, C. Moreno-Castilla, C.A. Costa, L.M. Madeira, Azo-dye Orange II degradation by heterogeneous Fenton-like reaction using carbon-Fe catalysts, Appl. Catal. B: Environ., 75 (2007) 312–323.
[30] F. Duarte, F. Maldonado-Hódar, A. Pérez-Cadenas, L.M. Madeira, Fenton-like degradation of azo-dye Orange II catalyzed by transition metals on carbon aerogels, Appl. Catal. B: Environ., 85 (2009) 139–147.

[31] K. Vimala, K.S. Sivudu, Y.M. Mohan, B. Sreedhar, K.M. Raju, Controlled silver nanoparticles synthesis in semi-hydrogel networks of poly (acrylamide) and carbohydrates: a rational methodology for antibacterial application, Carbohyd. Polym., 75 (2009) 463–471.
[32] T.A. Jelić, J. Bronić, M. Hadžija, B. Subotić, I. Marić, Influence of the freeze-drying of hydrogel on the critical processes occurring during crystallization of zeolite A–A new evidence of the gel "memory" effect, Micropor. Mesopor. Mater., 105 (2007) 65–74.
[33] W. Subramonian, T.Y. Wu, Effect of enhancers and inhibitors on photocatalytic sunlight treatment of methylene blue, Water Air Soil Pollut., 225 (2014) 1922.
[34] P. Malik, S.J.S. Saha, Oxidation of direct dyes with hydrogen peroxide using ferrous ion as catalyst, Separ. Sci. Technol., 31 (2003) 241–250.
[35] T. Shahwan, S.A. Sirriah, M. Nairat, E. Boyacı, A.E. Eroğlu, T.B. Scott, K.R. Hallam, Green synthesis of iron nanoparticles and their application as a Fenton-like catalyst for the degradation of aqueous cationic and anionic dyes, Chem. Eng. J., 172 (2011) 258–266.
[36] S.G. Huling, S. Hwang, Iron amendment and Fenton oxidation of MTBE-spent granular activated carbon, Water Res., 44 (2010) 2663–2671.
[37] S.-S. Lin, M.D. Gurol, Catalytic decomposition of hydrogen peroxide on iron oxide: kinetics, mechanism, and implications, Environ. Sci. Technol., 32 (1998) 1417–1423.
[38] E. Garrido-Ramírez, B. Theng, M. Mora, Clays and oxide minerals as catalysts and nanocatalysts in Fenton-like reactions—a review, Appl. Clay Sci., 47 (2010) 182–192.
[39] Z. Han, Y. Dong, S.J.J.o.h.m. Dong, Copper–iron bimetal modified PAN fiber complexes as novel heterogeneous Fenton catalysts for degradation of organic dye under visible light irradiation, J. Hazard. Mater., 189 (2011) 241–248.